2008

Comparison of Two Methods of External Scatter Dose Contributions to the Contralateral Breast

James Cutlip
Wright State University

Comparison of Two Methods of External Scatter Dose Contributions to the Contralateral Breast

A thesis submitted in partial fulfillment
of the requirements for the degree of
Master of Science

By

JAMES CUTLIP
B.S., Marshall University 2006

2008
Wright State University

WRIGHT STATE UNIVERSITY

SCHOOL OF GRADUATE STUDIES

June 23, 2008

I HEREBY RECOMMEND THAT THE THESIS PREPARED UNDER MY SUPERVISION BY James Cutlip ENTITLED Comparison of Two Methods of External Scatter Dose Contributions to the Contralateral Breast BE ACCEPTED IN PARTIAL FULFILLMENT OF THE REQUIREMENTS FOR THE DEGREE OF Master of Science

_____

Brent Foy, Ph. D.
Thesis Director

_____

Lok C. Lew Yan Voon, Ph. D.
Department Chair

Committee on
Final Examination

_____

Brent Foy, Ph. D.

_____

Paul Hanny, Ph. D.

_____

David Smith, Ph. D.

_____

Joseph F. Thomas, Jr., Ph. D.
Dean, School of Graduate Studies

Abstract

Cutlip, James. M.S., Department of Physics, Wright State University, 2008. Comparison of Two Methods of External Scatter Dose Contributions to the Contralateral Breast.

The treatment outcomes of many forms of breast cancer have become very favorable. The usual standard of successful treatment of five years without a recurrence is not adequate any longer for breast cancer. Many patients live well beyond this time interval only to have a second malignancy develop in the contralateral breast ten or twenty years later. Boice *et al* (1992) found that there was a correlation between the amount of dose to the contralateral breast and the likelihood of a secondary malignancy forming.

The normal practice today is to use multi-leaf collimators (MLC) to modulate the photon beam in radiation therapy. Due to the limited use of physical compensators, very little data has been presented as to their effectiveness in reducing dose to the contralateral breast. This study will use a Varian 2100 C/D linear accelerator to irradiate a Rando phantom with simulated breast material using both the traditional method and the compensator method. The dose to the contralateral breast will be measured using MOSFETs at various depths in the tissue.

The results suggest that the compensators do not reduce the dose to the contralateral breast as effectively as the MLC method. There were a few instances for specific cases where the compensator performed better and these cases require further study for verification and clarity.

Table of Contents

List of Figures

List of Tables

1. Introduction

Due to the advanced techniques in radiotherapy for the treatment of many cancers, which allow for much more efficient and effective delivery, new practices must be tested in order to ensure the best possible patient outcome. With the use of IMRT (intensity modulated radiation therapy), IGRT (image guided radiation therapy), stereotactic radiosurgery, compensators and other beam modulators, the management of cancerous cells has improved greatly with the benefit of sparing a great amount of normal tissue. One such cancer that has benefited from these advances is breast cancer. It was the common practice after diagnosis of this disease for a radical mastectomy. Recently another approach has been found to be just as effective for early stage breast cancer. This approach is a conservative surgery (i.e. lumpectomy) followed by radiotherapy. The long term survival data from a number of clinical trials comparing the two methods do not reveal any detrimental effects resulting from the use of radiotherapy (Arriagada 1996, Fisher 1995, Jacobson 1995, Veronesi 1995, van Dongen 2000). It is well known that radiation is a carcinogen; therefore it is of great importance to reduce the exposure to normal tissue while maximizing the dose to the targeted area(s). It is this principle of minimizing unwanted dose that has prompted many studies in the reduction of exposure to the contralateral breast.

In the beginning of the fight against cancer, it was often prudent to discuss one's survival in a five year time frame. The long term survival possibility was not often expected for many cancers. Since then many patients that have been diagnosed have gone on to live much longer than the previous five year window that was observed. This prolonged life outcome has lead for the need to ensure that the possibilities of second malignancies such as contralateral breast cancer are kept to a minimum. Many studies have shown that the risk of secondary cancers increases significantly with time after the initial treatment to the primary tumor. The increase in probability of developing contralateral breast cancer has been documented as 10% for 15 years and as much as 1% for each year for up to 20 years after the treatment of the diseased tissue with radiation therapy (Kurtz 1988, Obedian 2000, Gao 2003). Since the prognosis for early stage breast cancer is so promising, many of the patients will live long enough for the inherent increase in risk of secondary malignancies to come to fruition.

Due to the probable correlation between radiotherapy and contralateral malignancy, the principle of ALARA (as low as reasonably achievable) is the sole driving factor for these studies. It may not be that radiation increases the risk equally in everyone, but it is well worth reducing the dose for all that are susceptible to the added exposure.

The goal for this project is to compare two methods of minimizing the dose to the contralateral breast during radiotherapy. The use of a low Z material compensator (a custom shaped polymer placed in the path of the beam) will be compared to conventional half beam tangential therapy. The project entails using a human shaped phantom and two simulated breasts made of tissue comparable material to simulate the dose to the contralateral breast by the two techniques. The parameters that must be met in order for

an adequate comparison are that the dose to the target tumor be equal to the prescribed dose, the dose be homogeneous at the target location, and no normal tissue is compromised in order to satisfy the previous two. To ensure this, the isodose curves produced by both methods for each field will be compared for equality. It is hypothesized that the dose to the contralateral breast will be reduced using the compensator. This is based on the idea that radiotherapy using the compensator method will require less energy (fewer monitor units, MU's) to deliver the same dose to the target tissue, which should reduce the contralateral dose due to scattering.

2. Background and Theory

The process for the proper and precise delivery of radiation treatment consists of a complex series of events. These events must be controlled and monitored to ensure the prescribed dose is given as accurately as possible. The first control is established before any patient is ever treated. The radiation delivery unit, the linear accelerator (linac), must undergo extensive quality assurance tests. These tests keep the linac functioning within very precise parameters.

The treatment of a cancer patient begins when they visit the radiation oncologist. After a series of tests and diagnostic images (CT, MRI, etc.) are performed, the oncologist determines the stage of the cancer and a treatment plan; chemotherapy, surgery, radiation, or any combination may be administered. When radiation is the method chosen, the doctor gives a prescribed dose to treat the patient. This treatment may be a means to a cure or palliative.

Once the method of treatment and dose are prescribed, the images from the patient's CT scan are used to determine the contours of the critical organs and the cancerous growth(s). This is done using the treatment planning system (TPS) that corresponds to each individual linac. The limiting factor for the delivery of radiation is not how much the tumor can withstand. The factor that limits the dose is the normal tissue surrounding

the diseased area. Normal tissue can only be exposed to so much radiation dose before it cannot function properly. There are many reports that contain the therapeutic dose allowances for many normal tissues in the body. It tells the probability of normal tissue complications for given doses. For further explanation on this study please refer to the article by Emami *et al* in the *Int. J. Radiat. Oncol. Biol. Phys. 21: 109 –122.*

After the contours are drawn for the patient, the TPS is then used to determine the best delivery method for the prescribed dose. The TPS uses advanced algorithms to calculate the dose to the tumor and surrounding areas. The algorithms are based on percent depth doses and output factors that are determined during the commissioning of the system.

The finalized plan is then implemented by the radiation therapists. The therapists are responsible for patient set up consistency. They also take further images to track the tumor as the treatment continues.

Section 1: Background

2.1.1 Introduction to the Linear Accelerator (Linac)

The linac is a device that uses high frequency electromagnetic waves to accelerate charged particles to high energies through a linear tube. The particles that are accelerated are electrons and they can be used for treating superficial tumors or they can strike a target to produce x-rays for treating deep seated tumors. Figure 2.1 is a block diagram of a medical linear accelerator showing the major components and auxiliary systems.

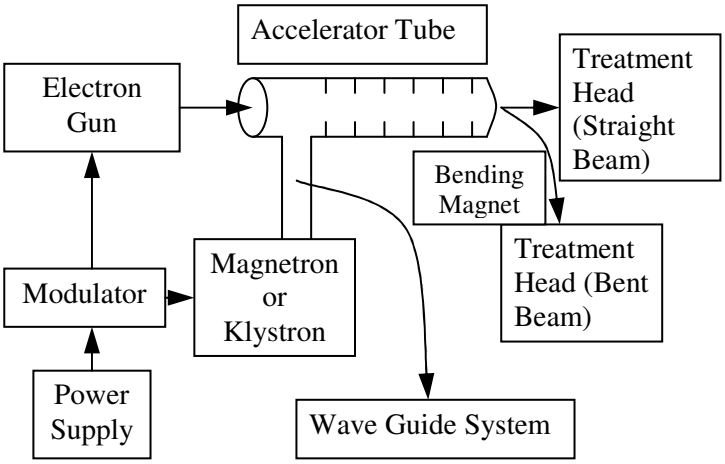

Figure 2.1: Block diagram of typical medical linear accelerator. (Taken from Khan 2003).

A power supply provides direct current power to the modulator. The modulator includes the pulse forming network. High voltage pulses from the modulator are delivered to the magnetron or klystron and simultaneously to the electron gun. Pulsed microwaves from the magnetron or klystron are injected into the accelerator tube via a waveguide system. Electrons from the electron gun are also injected into the accelerator tube in a pulsing manner. The electrons gain energy from the sinusoidal electric field. As the high energy electrons exit the accelerator structure, they are in the form of a pencil beam about three millimeters in diameter.

2.1.2 Treatment Head

Once the electron pencil beam exits the accelerator tube it enters the treatment head. Figure 2.2 shows the components of the treatment head for the use of electrons and x-rays.

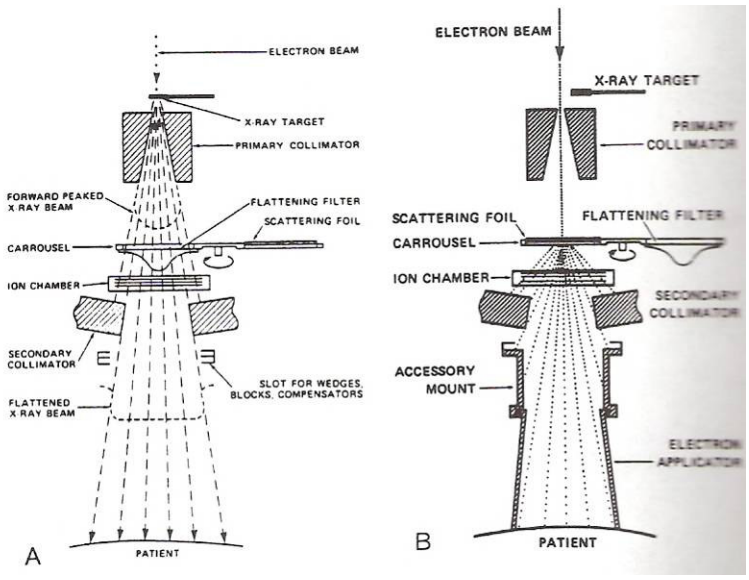

Figure 2.2: Components of the Treatment Head. A: X-ray therapy mode. B: Electron therapy mode. (Taken from Khan 2003).

The treatment head consists of an x-ray target, scattering foil, flattening filter, ion chamber, fixed and movable collimator, and light localizer system.

Not all of these components are used at once. The target and flattening filter are only used when it is desired to use the x-ray therapy mode. The flattening filter is used to make the beam intensity uniform across the field. The scattering foil is only used for electron therapy mode to disperse the three mm pencil beam (Khan 2003).

Section 2: Breast Cancer Treatments

2.2.1 Conventional Two Beam Open Field Set-up

The most common set-up for breast cancer patients is a two field x-ray approach with the patient supine, ipsilateral arm above head (Murshed 2006). The first field is the medial tangent field and the second is the lateral tangent field. The medial tangent field involves the linac gantry to be positioned over the patient and slightly off to one side so the beam can enter the breast at a tangential angle. The lateral field has the gantry

positioned off to the ipsilateral side and slightly below the table level. Figure 2.3 shows an example of the fields for two beam open field therapy.

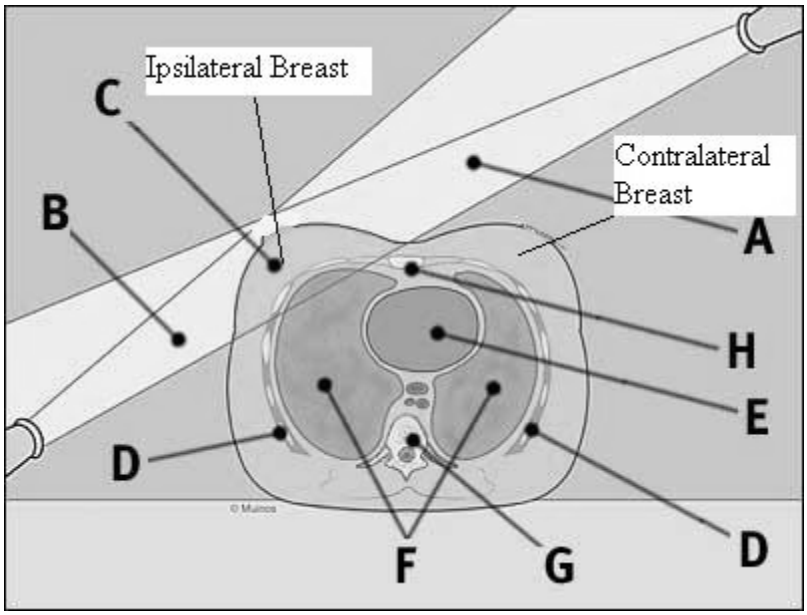

Figure 2.3 Open field Therapy. A-medial tangential beam, B-lateral tangential beam, C-target breast, D-rib cage, E-heart, F-lungs, G-spine, and H-sternum. (Taken from praning5254.blogspot.com).

2.2.2 Two Field Half Beam Blocking Set-up

For this technique the same gantry angle methods are used as the open field technique. Now instead of having the full field, the collimators are used to block out one complete half of the field. This is done in an effort to minimize the dose to the internal organs such as the lung and heart. As seen in Figure 2.3, the lung is getting dose from the initial field. Figure 2.4 shows an example of half beam blocking and the resulting dose curve.

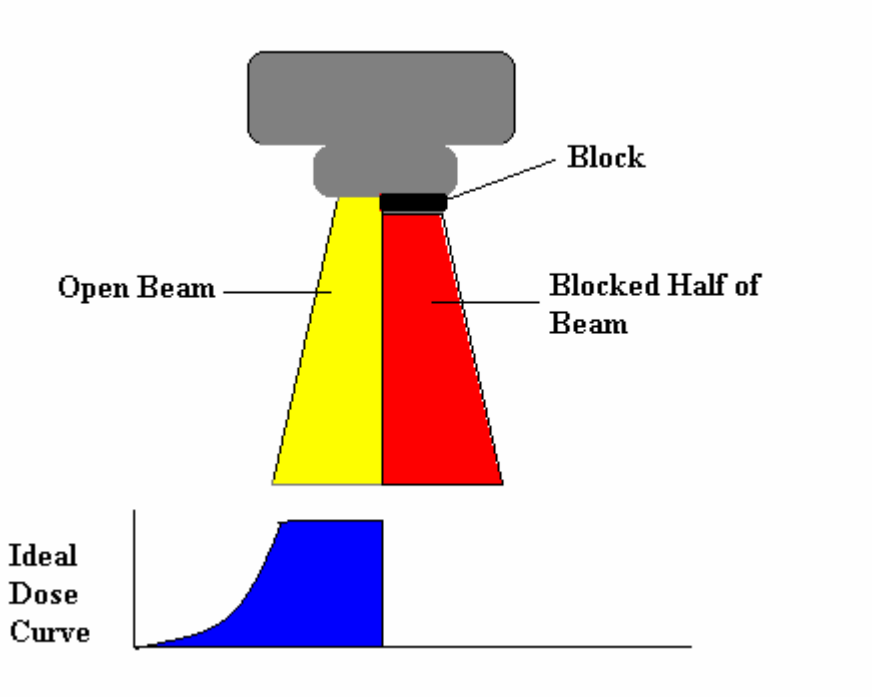

Figure 2.4: Half Beam Blocking

2.2.3 Intensity Modulated Radiation Therapy Delivery

Linacs normally generate x-ray beams that are flattened and collimated by four movable jaws to produce rectangular fields. The dose rate can be changed uniformly within the beam precollimation, but not spatially. That is the entire beam can be altered, but not small portions of the beam. To produce intensity modulated fluence profiles, precalculated by the TPS, the linac must be assisted with a system that can change the given beam profile into that of an arbitrary shape. Many classes of intensity modulated systems have been devised including: wedges, compensators, and multileaf collimators (Khan 2003).

2.2.3.1 Wedges

The wedge is an absorbing block placed in the path of the beam to modify its isodose distribution (fluence). The wedge causes a progressive decrease in the intensity across

the beam, resulting in a slope of the isodose curves from their normal positions. Figure 2.5 and Figure 2.6 represent normal isodose curves and those from an introduced wedge.

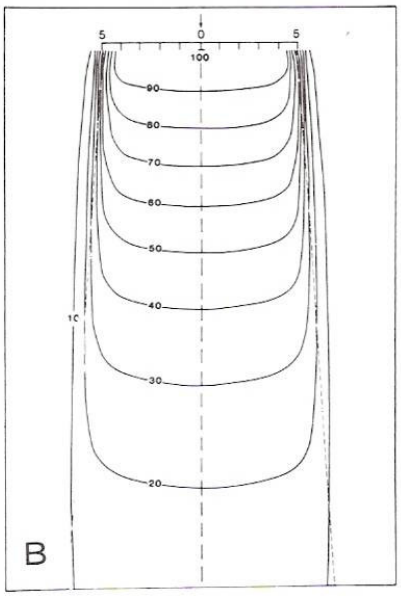

Figure 2.5: Normal Isodose Curve. (Taken from Khan 2003).

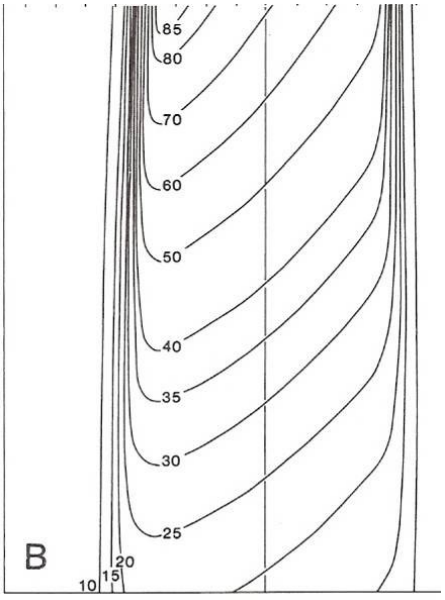

Figure 2.6: Isodose Curve with Wedge in Beam. (Taken from Khan 2003).

Wedges are placed in the beam path, but they are placed far enough away from the patient to allow for skin sparing. Wedges are used for sloping surfaces where the contour of the surface can be approximated as straight line (Khan 2003).

2.2.3.2 Compensators

Missing tissue compensators are used for radiation beams incident on an irregular surface. The compensator corrects the non-uniformity of dose to the target volume caused by the irregular surface. The compensator also helps to deliver a homogeneous dose to an irregularly shaped tumor. That is a tumor that is not uniformly shaped and rather large so as to not receive a uniform dose due to it having features far from the center of the field. Figure 2.7 demonstrates the use of a missing tissue compensator (Khan 2003).

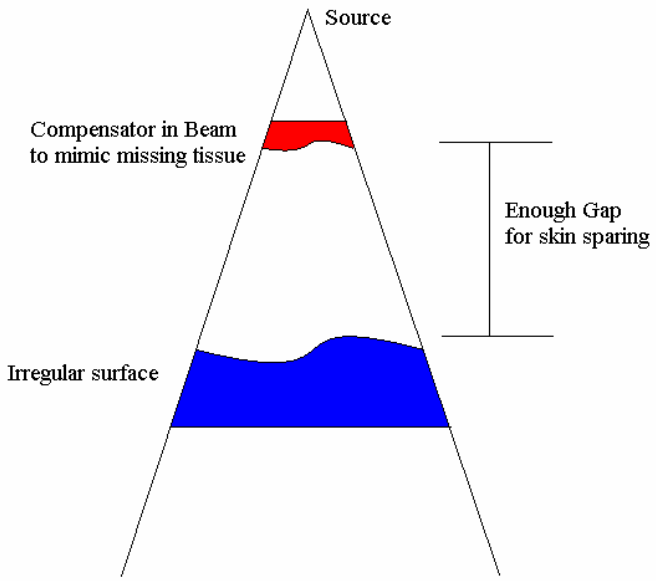

Figure 2.7: Compensator Placement

2.2.3.3 Multileaf Collimators (MLC)

MLCs for x-ray beams consist of a large number of collimating leaves that are driven automatically and independent of one another. This allows for the generation of a field of

any shape. MLC's can be used as a stationary collimator window or can move and modulate the beam. Figure 2.8 gives a view of an MLC set to a non-rectangular shape.

Figure 2.8: MLC. (Taken from homepage.mac.com).

The picture represents the stationary use of the MLC, but the MLC can be dynamic. This characteristic allows the beam to be corrected for missing tissue and tumor shape deformities. The first dynamic method utilized by the MLC is called a "step-and-shoot." It uses subfields in order to modulate the beam's intensity over a volume. The linac beam is not on when the field is changed. It is implemented by irradiating a volume, stopping and changing the field, and irradiating again. There is also a "dynamic-step-and-shoot" that allows the beam to be on while the MLC's go from one set field to another.

The second dynamic MLC delivery method allows the leaves to sweep simultaneously at different velocities to achieve the fluence predetermined by the TPS. This method is referred to as the "sliding window." It is advantageous in that it requires less time than the step-and-shoot method and it is very versatile for many conditions. Figure 2.9 demonstrates this approach for a single leaf pair of the MLC. (Khan 2003).

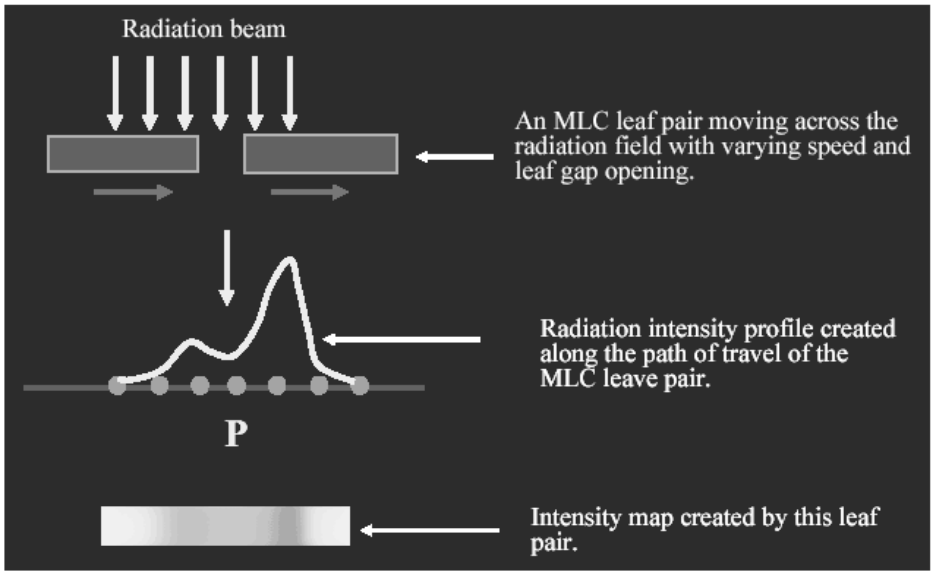

Figure 2.9: Illustration of dynamic MLC for Intensity Modulated Radiation Therapy. (Taken from www.biij.org).

Section 3: Radiation Production and Interaction

2.3.1 X-ray production

X-rays are produced by accelerating electrons into a metallic target. The energy of the generated x-ray depends on the energy of the incident electron. There are two mechanisms responsible for the production of x-rays: Bremsstrahlung and characteristic x-rays.

Bremsstrahlung is the result of an interaction between an electron and the magnetic field of the target's atoms. As the electron passes the atom, the magnetic field acts on the electron causing it to deflect from its original path and lose some of its kinetic energy. In the process of deflection, a photon is emitted whose energy depends on the Z (electron density) of the target material and the kinetic energy of the incident electron. The greater the number of electrons, the greater the probability there will be an interaction.

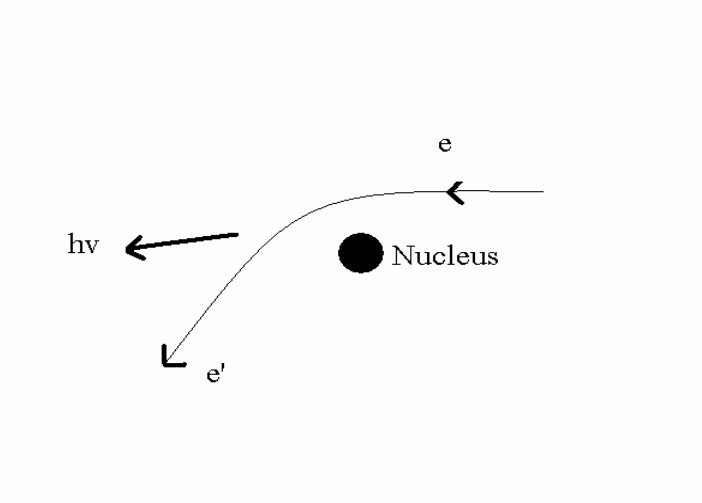

Figure 2.10: Bremsstrahlung Production. (Taken from Khan 2003).

Characteristic x-rays are produced when an incident electron interacts directly with the orbital electrons of the target material. If the energy of the incident electron is great enough (greater than the binding energy of the orbital electron), the orbital electron is displaced causing the atom to become ionized. The vacancy of the displaced inner shell electron is then filled by one of the outer shell electrons and a photon is emitted with an energy equal to the difference of the two orbital electron energies. The process of characteristic x-ray production is illustrated in Figure 2.11 (Khan 2003, Attix 1986).

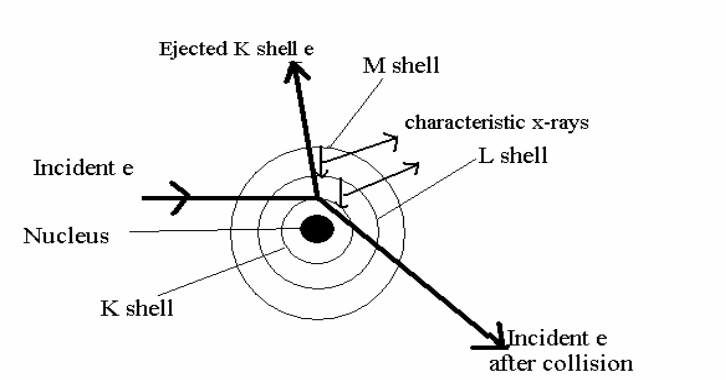

Figure 2.11: Characteristic X-ray Production. (Taken from Khan 2003).

2.3.2 X-ray Interaction with Matter

X-rays interact with matter primarily in four ways: photoelectric effect, coherent scattering, Compton scattering, and pair production. The photoelectric effect is not seen in the megavoltage energy range for x-rays. Coherent scattering is also present in much lower energies than those for radiation therapy. The two processes that must be accounted for here are the Compton scatter and pair production.

Compton scatter is the dominant interaction process in the megavoltage region. The interaction that occurs is between an incoming photon and an electron. The energy of the photon is much greater than the binding energy of the electron. The photon interacts with the electron imparting energy onto it (as much as the incident photon's energy). The electron is then scattered if enough energy was delivered at some angle φ and the photon is deflected at some angle θ. Compton scatter is responsible for most of the uncertainty in the delivery of dose to normal tissue. One of the main sources for this scatter is produced from the collimator itself. Although most of the beam is contained within the field, some of the x-rays are able to escape by the nature of the process. These rogue x-rays can cause dose to be delivered outside the area of interest. Most of these x-ray doses are insignificant but there are times when they need to be considered as in the case of the scattered dose to the contra lateral breast. Compton scatter can also occur within the body itself. The scatter does not always work in favor of dosimetry. In the case again of dose to the contra lateral breast, x-rays can scatter off of the chest wall (bone) or other features and be directed to the healthy breast, lung, or heart. Of these two scattering methods, the collimator scatter seems to be the easiest and most important scatterer to minimize.

The final interaction that occurs is pair production. This process requires a minimum of 1.022 MeV of energy. This corresponds to the mass of energy of an electron which is 0.511 MeV. In pair production a photon of energy greater than or equal to 1.022 MeV interacts with an electromagnetic field of a material producing an electron and a positron pair that are emitted at two different angles and usually in the same forward direction as the photon. Any additional energy is converted into the kinetic energy of the electrons. This process relies heavily on the Z of the material and is proportional to the Z^2. The human body mainly consists of tissue comprised of water which has a low Z; therefore this process is not very abundant in radiation therapy.

These x-ray processes are not directly ionizing. That is they do not produce chemical and biologic damage themselves, but when they are absorbed in the material through which they pass. When absorbed by the previous processes, they produce fast moving charged particles that in turn are able to produce damage (Khan 2003, Attix 1986, Hall 2006).

2.3.3 Electron Interaction with Matter

Electrons, on the other hand, are directly ionizing. Electrons can have a direct or indirect action on the matter they are in contact with in the human body. In the case of radiation to the human body, direct action occurs when a photon is absorbed and an electron is displaced. This electron now interacts with the DNA to produce an effect. Indirect action occurs from the interaction of a displaced electron that interacts with another molecule and causes that molecule to interact with the DNA. An example of that is when the electron interacts with a water molecule to produce a hydroxyl radical. This radical then causes the damage to the DNA structure. The reader is referred to

Radiobiology for the Radiologist by Eric J. Hall for further in depth explanation of the photon and electron interaction with matter (Khan 2003, Attix 1986, Hall 2006).

Section 4: Measuring Radiation

In the early stages of radiation therapy using x-rays, attempts were made to measure ionizing radiation on the basis of chemical and biologic effects. For instance, radiation effects on photographic emulsions, changes in color of some chemical compounds, and reddening of the human skin could be related to the amount of radiation absorbed. However, these were only able to give very crude estimates at the time. Also, at this time the ranges of energy for therapy were in the orthovoltage range (~200-300 kV); at these energies the skin was the limiting organ and targets were within two centimeters of the skin's surface. With current energies in the megavoltage range and the effective depths of treatment much deeper (thus delivering less dose to the skin) the time it would take for the skin to redden would be much greater and the damage to other organs and tissues much more severe. A new method of measuring had to be issued due to this skin sparing effect of the megavoltage energies (Khan 2003).

2.4.1 The Roentgen

The Roentgen is a unit of exposure. Exposure is a measure of ionization produced in air by photons. The International Commission on Radiation Units and Measurements (ICRU) defines exposure (X) as the quotient of the dQ by dm where dQ is the absolute value of the total charge of the ions of one sign produced in air when all the electrons (negatrons and positrons) liberated by photons in air of mass dm are completely stopped in air: $X = dQ/dm$. The Systems Internationale d'Unites (SI) unit for exposure is

coulomb per kilogram (C/kg) but the special unit is roentgen (R). 1R = 2.58E-4 C/kg air (Khan 2003).

2.4.2 Absorbed Dose

The problem with radiation exposure is that it only describes the ionization produced in air and not the amount in tissue or some other medium. Also, radiation exposure only applies to photons and not to protons, neutrons, or heavy ions and cannot be used for photon energies above 3 MeV. The quantity, "absorbed dose," has been defined to describe the quantity of radiation for all types of ionizing radiation, including charged and uncharged particles, all materials, and all energies. Absorbed dose (or just dose) is the quotient of *dE/dm*, where *dE* is the mean energy imparted by the ionizing radiation to material of mass *dm*. The traditional unit for dose is the rad (radiation absorbed dose). It represents the absorption of 100 ergs of energy per gram of absorbing material.

$$1 \text{ rad} = 100 \text{ ergs/g} = 10^{-2} \text{ J/kg}$$

The SI unit for dose is the gray (Gy). It is defined as 1 J per kg.

$$1 \text{ Gy} = 1 \text{ J/kg}$$

Thus, the relationship between the rad and Gy is:

$$1 \text{ rad} = 10^{-2} \text{ Gy} = 1 \text{ cGy}$$

Dose is measured in material (usually a water phantom) and the depth along the central axis at which the maximum dose, D_{max}, is recorded is defined as the d_{max} or d_0. This is a reference depth that is used to calculate the dose anywhere in the material. The relationship utilized here is called the percent depth dose (P). It is defined as:

$$P = \frac{D_d}{D_{d_0}} \times 100$$

Where D_d is the dose at some depth, d, and D_{d0} is the reference dose usually found to be the depth at maximum dose. A number of parameters affect the central axis depth dose distribution such as beam energy, depth, field size and shape, source to surface distance, and beam collimation.

The linac output is calibrated to deliver one monitor unit per rad (10^{-2} Gy or 1 cGy) at a reference depth for a specific field size and source to calibration point distance (Khan 2003).

Section 5: Tools for Measuring Dose

There are many tools used to measure the absorbed dose. Some of the tools allow for the measurement *in-vivo* while others only allow for phantom measurements. The most prominent tools for measuring dose are ion chambers, thermo luminescent dosimeters, MOSFETS, and diodes. All have their own advantages and disadvantages.

2.5.1 Ion Chambers

Ion chambers are designed for the use of machine calibration and monitoring for linacs that operate in the megavoltage range. These chambers must also be calibrated yearly; that requires a facility that has a free air ionization chamber. The free air ionization chamber is a very delicate and bulky chamber that cannot be used for routine measurements in the clinic. The free air chamber is an instrument used in the measurement of the roentgen according to its definition.

There are different types of ion chambers. The practical ion chamber requires a few key characteristics. First, there should be minimal variation in sensitivity over a wide range of photon energies. The chamber should also be independent of the direction of incident radiation. The voltage in the chamber should be high enough for optimal

recombination so that electronic equilibrium is satisfied; otherwise, ions recombine before contributing to the measured charge. Lastly, the ion chamber must be calibrated for exposure against a standard measurement for all radiation qualities of interest.

The ion chamber is an excellent tool for measuring many outputs of the therapeutic linac in terms of exposure, but it has its limitations for measuring dose in a human. Correction factors are applied to the measurement to calculate the dose in phantoms. The ion chamber is limited in that it is not very effective in measuring *in vivo* dosimetry for human patients due to its high voltage bias and large size compared to other methods of dosimetry (Khan 2003).

2.5.2 Thermo luminescent dosimeters

Thermo luminescent dosimeters (TLDs) are crystalline materials that emit light when they are heated after irradiation. When the crystal is irradiated, a very minute fraction of the absorbed energy is stored in the crystal lattice. Some of this energy can be recovered later as visible light if the material is heated. The phenomenon of the release of visible photons by thermal means is known as thermo luminescence (TL).

The process of reading measuring the TL output starts with heating the irradiated material. The emitted light is measured by a photomultiplier tube (PMT) which converts light into electrical current. The current is then amplified and measured by a counter.

There are several TL phosphors available but the most common is lithium fluoride (LiF). Lithium fluoride has an effective atomic number of 8.2 compared with 7.4 for soft tissue. This makes the material a reliable tool to use for dose comparisons in clinical dosimetry.

TLDs are used to monitor the dose to radiation personnel. Properly calibrated TLD's can achieve a two percent uncertainty and are very effective as a secondary way of measuring linac output. The TLD are exposed to an amount of monitoring units and shipped to special centers where the dose can be measured.

2.5.3 MOSFETS

MOSFET stands for metal-oxide semiconductor field-effect transistor. MOS transistors present advantages such as low cost, small volume and weight, robustness, accuracy, large measurable dose range, and sensitivity to low-energy radiation (10 keV). They are useful in real-time measurements or post-irradiation read-out, while they retain information after reading. The sensitivity of unbiased MOSFETs has been improved, and further improvement is possible by increasing the oxide thickness via dual dielectrics or by using ion-implanted oxides and stacked MOSFET configurations. The stacked-transistor configuration is a very promising solution to reach the mRad range (personnel dosimetry). MOSFETs are already used in various application fields with increasing interest for use in specific cases of in-vivo dosimetry (IEEE 1998).

Figure 2.12: MOSFET detectors.

Figure 2.13: Reference to the Size of the MOSFETs.

2.5.4 Diodes

Silicon p-n junction diodes are often used for relative dosimetry. There are distinct advantages to using diodes such as high sensitivity, instantaneous response, small size, and durability. The main disadvantages are that they are energy dependant in photon beams, directional dependence, thermal effects, and radiation induced damage. Although modern diodes for medical dosimetry have minimized these effects, they are still present and cannot be completely ignored.

Diodes are very useful for patient dose since they can be taped directly to the patient at suitable points to measure dose. The diodes are carefully calibrated to provide a check of patient dose at a reference point. Calibration factors are applied to convert the diode reading into expected dose at the reference point. These factors take into account source-to-detector distance, field size, and other parameters used in the calculation of monitor units.

Section 6: Previous Studies

2.6.1 Contralateral Breast Risk

There have been many studies in regard to contralateral breast cancer. The two main areas of study are who is at risk and how to reduce the dose to the non-affected area.

Regarding who is at risk the only factor that has shown a link to increased contralateral breast cancer to radiotherapy is age (Burmeister 2008). Boice *et al.* (1992) examined the effect that the patient's age has in the risk of developing second malignancies after radiation therapy treatment. The study concluded the relative overall increase in risk of contralateral breast cancer after the treatment for the primary target by radiation was 1.19. It was also found that the relative risk was 1.59 for patients under the age of 45 at the time of the treatment and this increased to 1.85 for 10 year survivors who were under the age of 45 at the time of the treatment. Gao *et al.* (2003) showed a relative risk of 1.32 for patients under 45 as well as a risk of 1.15 for patients over 55. These studies all suggest that the younger the patient was at the time of the radiation treatment, then the greater the risk that they may develop a secondary malignancy in the contralateral breast. However, Obedian *et al.* (2000) found 15 year follow up rates for patients under 45 of 10% for conservative surgery followed by radiotherapy and 7% for patients undergoing radical mastectomy. It was concluded in the study that the increase was not statistically significant. Although the direct correlation between second malignancies and radiotherapy is not fully known and still under debate, it is a prudent practice to minimize any factor that may cause an increase in risk.

2.6.2 Minimizing Contralateral Breast Dose

Kelley *et al.* (1996) reported a study of four different techniques with a 6 MV linac beam. Using the Rando phantom and TLDs, they set up the beam arrangements as half beam with custom blocks, half beam using asymmetric collimator jaws, half beam using asymmetric collimator jaws with custom blocks, and isocentric technique with non

divergent posterior border. They observed the highest dose for the medial field with a wedge and the lowest with asymmetric jaws and no medial wedge or block.

Bhatnagar *et al.* (2004) reported comparison of IMRT and conventional tangential field technique with wedges. They observed the contralateral breast dose of 7.24 ± 2.35% of the primary breast dose (5000 cGy) in IMRT and 9.24 ± 2.04% of the primary dose using the conventional tangential field technique. This shows a 20% reduction on dose to the contralateral breast dose (362 cGy IMRT and 462 cGy conventional).

Muller-Runkel *et al.* (1990), Sohn *et al.* (1999), and Goffman *et al.* (2004) utilized in various methods lead shielding to reduce the dose to the contralateral breast. All showed a reduced dose in their studies. These reductions ranged from one third to one half of the original measured dose to the contralateral breast.

Chougule *et al.* (2007) used a Co-60 unit to measure the dose to the contralateral breast for numerous patients. It was concluded that the dose generated by the medial tangential field was almost twice as much as the lateral tangential field. It was also postulated that a considerable amount of the dose from the lateral field was due to internal scatter and the dose from the medial field was primarily attributed to the scatter from the collimator.

A recent study described the incorporation and comparison of many of the techniques previously mentioned. The studied was performed by Burmeister *et al.* (2008) using a Varian 2300 EX linear accelerator with a 6 MV beam. The study measured the absorbed dose on the surface and inside the contralateral breast in a phantom using treatment plans delivered 5 different common ways. These included medial and lateral paired wedges, a lateral wedge only, custom fabricated compensators, aperture based (field-in-field) IMRT

in which the segments are chosen by a leaf-sequencing algorithm after dose volume histogram based fluence map optimization. Also, various thicknesses of lead shielding were used for each method to further reduce the scattered dose. This is the only study found that utilized a complete physical compensator instead of a wedge. The compensator was composed of bismuth polyethylene (80% Bi, 19.2% PE). The group fabricated 2 wax breasts to simulate human tissue and placed them on a Rando phantom. Measurements from multiple locations on and inside the breast were taken. Looking at Table 2 in the report, it is shown that the monitor units are the greatest for the compensator. Referring to Table 4 in the report, the percent of the total dose delivered to the contralateral breast by the compensator method is second to worst only to the paired wedge method for internal absorbed dose and the worst for surface absorbed dose (Burmeister 2008).

While the project by Burmeister *et al.* (2008) is very complete it is worth noting the composition of the compensator. The density of the compensator composed of over 80% of bismuth is fairly high. Since bismuth makes up a vast majority of the composition of the substance it would seem that it raises the effective Z to a relatively higher number. This would result in a higher absorbed dose to the contralateral breast.

3. Methods and Materials

Section 1: Building a Compensator

3.1.1 The Milling Process

The process of building the missing tissue compensators involved the use of Varian's Eclipse treatment planning system, MATLAB® and C++®, the milling machine, and the compensator materials. This was a time consuming process that consisted of bridging the language gap between the treatment planning system (TPS) and the milling machine as well as time for physical milling, pouring and setting of the compensator material. The TPS generates a fluence map that is represented as an m-by-n matrix. Each element of the matrix represents an energy (dose) level. The map itself is analogous to a topography map of a geographic terrain. The lines on the fluence map represent isodose curves. These curves are used to determine if enough dose is being delivered to the targeted disease as well as ensuring there are not "hot spots" created that could cause harm to the patient's normal tissue due to overdosing.

Once the optimal fluence map is obtained for a given patient, the matrix representation of the map is exported from the TPS to MATLAB where it is first changed from an m-by-n matrix to an n-by-n square matrix. This is done due to the software requirements of the milling machine. It simply entails padding or erasing zeros from one side of the

matrix. The delivery technique being used for this analysis was half beam blocking, so erasing unnecessary zeros that would result in maximum drilling depth and ultimately excess Gypsum waste was done. This does not compromise the integrity of the dose to the primary disease.

Once the matrix is formatted into the appropriate dimensions, each element is then run through a previously determined attenuation/transmission formula. The transmission function previously mentioned was found by measuring the attenuation of the beam intensity through different thicknesses of the Gypsum material for the same field size. The transmission coefficient is equal to the inverse of the linear attenuation coefficient. The energy for all of photon beam was 6 MV; this is very important because different beam energies are attenuated differently. The initial beam intensity was referenced to be after the beam passed through the compensator tray and not before the tray. These measurements were used to calculate the transmission and then plotted and a best fit curve applied. This is the function that was applied into the MATLAB code.

This generates a new matrix of the same size that is used to determine the physical depth the milling machine will score. The new matrix must also undergo another transformation into a form that the milling will recognize. Instead of an n-by-n matrix, the milling program is designed to recognize each element by an x, y, and z coordinate system where x and y determine the location to drill by length and z is the actual depth. This process was performed using C++ in Visual Basic Editor. The x and y parameters are calculated from the field size that is to be on the patient. They are determined by where they are positioned in the beam by using similar triangles and geometry as demonstrated by Figure 3.1.

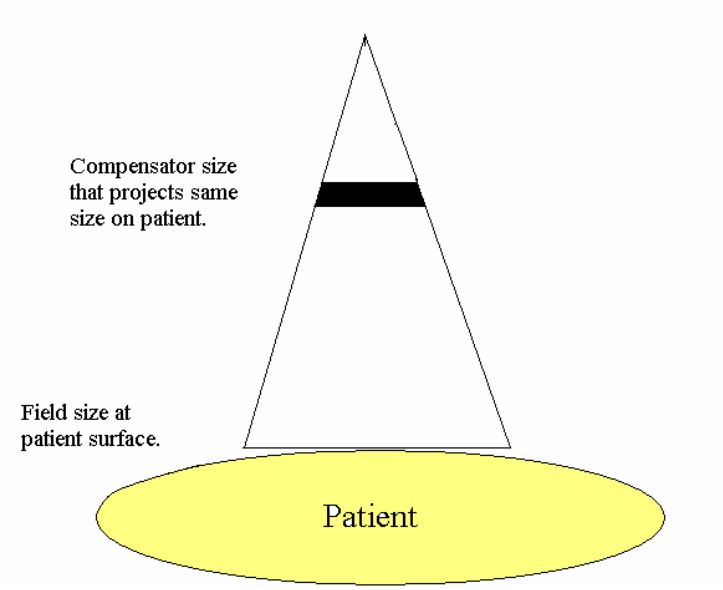

Figure 3.1: Example of Compensator Size Determined By Triangles Using Field Size on Patient Surface

The depth component is found by calculating how much material is needed so that a certain percent of the beam's energy (dose) is transmitted. The percent is normalized so the maximum is 100 %.

Once the matrix has been configured into the *xyz* matrix, it can be imported into the milling program. The program then generates a sample of the compensator given the data and then on command begins drilling row by row to the depth needed. The precision of the depth is determined by the drill bit width. The program does not allow for the bit to go too deep if it means that another coordinate would be compromised. In this case if the depth needs to be near absolute, a narrower bit must be used. The bit used had a 1/8" diameter. Figure 3.2 shows a milled compensator. The top half of the milled area is the area to be exposed to the beam. The sharp drop off is the edge where the beam was half blocked. The bottom part is to be blocked in order to conserve the more expensive Gypsum. It is not to be in the beam and there is no need to use and waste the material.

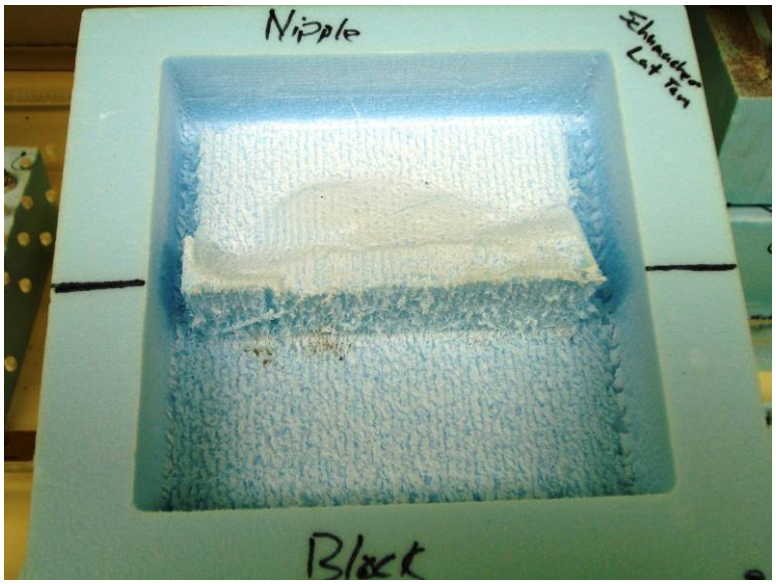

Figure 3.2: Milled Compensator

When the foam has been drilled, the Gypsum was added. The Gypsum is a compound similar to concrete in the method of mixing. It requires about a 1:1 mixture of material to water. After pouring into the Styrofoam molds (blocking the areas where the maximum depth is to conserve material so that only the area exposed to the beam is being covered), it takes a few hours or even a day to completely set up. Then when the Gypsum is ready, a small area is cut out from around the edge and also where the mounting screws will be. Now the blocked area is removed and the rest of the opened area is filled with Cerro bend. The Cerro bend is much more dense and attenuates much more than the Gypsum. The relative Z for the Cerro bend is not large enough that it will contribute to the dose significantly by particle interaction. Figure 3.3 shows a ready to mount and use compensator.

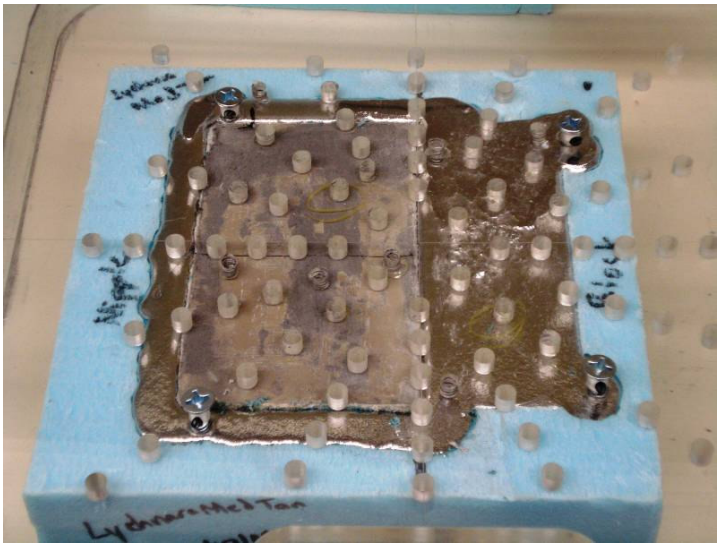

Figure 3.3: Completed Compensator Mounted on Tray

3.1.2 Testing the Fluence of the Compensator

After all of the compensators are built they are tested for comparison with the optimal fluence map generated by the TPS. The fluence map for the compensator is generated by the Mapcheck device. This device is a flat phantom that using numerous detectors to measure the fluence of a field. The fluence map must be within a certain tolerance range (3-4%) of one another for the compensator to be valid. The comparison is done on a point by point inspection using the Mapcheck software.

Section 2: Finding the Dose to the Contralateral Breast

The compensators are then used to test the dose to the contra lateral breast once they are proven to deliver the correct dose and fluence. This test is performed using an anthropomorphic phantom (Alderson Rando Phantom). It is a transversely sectioned phantom that enables dosimetric studies. Rando is built to allow the placement of dose measuring devices inside the body to mimic real life scattering and phenomena. Figure 3.4 is an example of the Rando phantom torso.

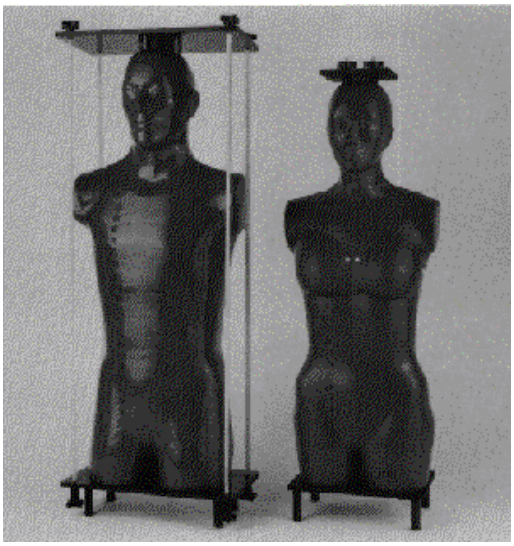

Figure 3.4: Alderson Rando Phantoms. (Taken from Khan 2003).

The figure shows the full torso and head set up for male and female phantoms, but for this experiment only the chest portion will be used. Also, the phantom available is the male version, so breasts of proper density were constructed and attached. The simulated target breast was constructed of a water filled bag. Water interaction with photons is very similar to tissue interaction with photons since the human body consists of over seventy percent water. The contralateral breast was constructed out of a material called super-flab. It also has a density very close to tissue. It was used because it comes in sheets of different thicknesses and the MOSFETs can be placed in between them (See Figure 3.6).

The phantom is then placed on the table and the procedure for the patient that the compensator was constructed from is reproduced. The parameters and set up are conserved for comparison accuracy for each patient and beam. MOSFETs are placed in the phantom in various locations to test the dose throughout the contra lateral breast to measure the inherent dose. An ion chamber is placed in the primary disease site to ensure

the prescribed dose was delivered. Figure 3.5 shows an example of the set up for the procedure.

Figure 3.5: Set Up for Medial Field (top) and Lateral Field (bottom) with Compensator

Using multiple MOSFET dosimeters provides a well defined dose distribution throughout and gives a numerical representation of where the majority of the dose is placed and from which beam. Placement of the MOSFETs is important as to ensure an accurate portrayal of the dose distribution. Areas of interest include the nipple, the surface adjacent the primary disease, the surface farthest from the tumor site, and areas in the center of the breast. The distribution of the dosimeters is shown in Figure 3.6. All of the MOSFETs

are placed approximately 3 cm inside the overlapping breast material except the one on the surface which will give a representation of the dose to the skin (super-flab).

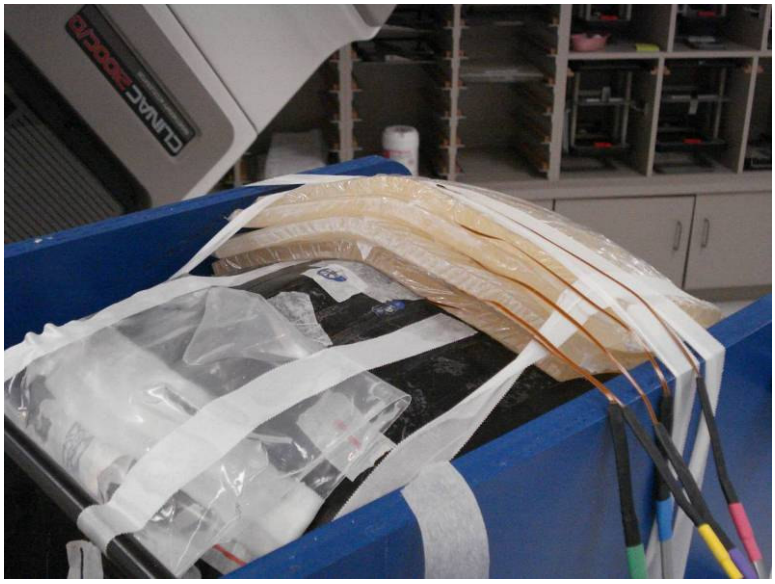

Figure 3.6: Rando with MOSFETs and Fabricated Breast Material

For all of the treatment plans, the method of treatment involved using half beam blocking with a 6 MV photon beam for both the lateral tangential beam and the medial tangential beam. The 6 MV photon energy was selected (as opposed to the 18 MV energy) due to the fact that at energies above 10 MV, there is a high generation of neutron dose that is created by the greater energy. The gantry and table positions, source to surface distance, and beam energy were all used for the comparable compensator approach. The MU setting, however, had to be lowered in order to match the prescribed dose. Every plan required two compensators (one for the medial field and one for the lateral field); there were six plans so a total of twelve compensators constructed. Each compensator was then tested using the method described. If any physical element of the treatment plan were to change such as the gantry position, collimator position, or table position, then a new compensator would have to be constructed for the changes.

The results of the tests are to be analyzed using a paired T-test statistical approach. The tests do not hold either of the methods performed as the control; rather it tests to see if there is a statistical difference between the two data sets. There were four T-tests performed for the data. The first test examines if the location/depth of the MOSFET influences the dose due to external scatter to the contralateral breast. The second test looks to see if the treatment plan has a deciding factor on which method reduces the dose to the contralateral breast. The third test analyzes the data to see if there is any influence on the field itself. It tests to see if data from the medial and lateral fields for the compensator are statistically different from the data from the MLC. The last test encompasses all of the data; it compares the complete set of data for the compensator against that of the MLC. The T-test values are determined to be statistically significant if $p < 0.10$. This implies that there is only a ten percent chance that the values are not equal. This is a lenient threshold but will allow for accurate enough analysis for the comparison of the dose to the contralateral breast.

4. Results and Discussion

Section 1: The Recorded Dose to the Contralateral Breast

The measured value from the MOSFETs is actually an accumulated voltage measurement in mV. Each MOSFET has a voltage (mV) to dose (cGy) conversion factor that must be implemented for each value. Table 4.1 displays the conversion factors for the MOSFETs used in the experiment.

MOSFET 1	2.98 mV/cGy
MOSFET 2	3.00 mV/cGy
MOSFET 3	3.71 mV/cGy
MOSFET 4	2.51 mV/cGy
MOSFET 5	2.98 mV/cGy

Table 4.1: Conversion Factors for MOSFETs.

Table 4.2 shows the calculated dose to the contralateral breast for six treatment plans consisting of the medial and lateral fields for both compensators and MLC.

	Dose in cGy to Contra Lateral Breast					
Mosfet #	1 Medial(MLC)	2 Medial(MLC)	3 Medial(MLC)	4 Medial(MLC)	5 Medial(MLC)	6 Medial(MLC)
1	1.01	111.74	193.96	115.10	1.01	125.50
2	1.00	122.33	209.33	127.00	1.33	126.67
3	0.81	110.24	181.40	113.48	0.54	113.48
4	5.18	227.09	366.53	223.11	1.99	205.58
5	5.03	106.71	158.05	93.29	10.40	91.95
	1 Medial(Comp)	2 Medial(Comp)	3 Medial(Comp)	4 Medial(Comp)	5 Medial(Comp)	6 Medial(Comp)
1	3.02	108.72	208.72	114.43	3.69	121.48
2	3.67	113.67	227.67	121.67	4.33	126.33
3	2.96	104.85	202.43	109.70	3.50	109.43
4	10.36	211.95	390.44	216.73	7.97	202.79
5	7.38	102.01	175.84	94.63	21.48	93.62
	1 Lateral(MLC)	2 Lateral(MLC)	3 Lateral(MLC)	4 Lateral(MLC)	5 Lateral(MLC)	6 Lateral(MLC)
1	1.01	39.26	52.68	34.23	74.50	47.32
2	1.33	34.33	50.33	29.67	69.67	37.67
3	0.54	25.61	37.74	25.61	48.52	26.95
4	0.00	47.81	65.34	43.03	69.72	44.62
5	0.00	32.21	41.95	29.19	54.03	33.56
	1 Lateral(Comp)	2 Lateral(Comp)	3 Lateral(Comp)	4 Lateral(Comp)	5 Lateral(Comp)	6 Lateral(Comp)
1	0.67	37.58	65.10	26.51	77.85	43.29
2	1.00	37.33	57.33	29.67	76.33	38.00
3	0.54	28.30	43.40	21.83	57.41	34.23
4	3.98	49.80	74.10	35.06	71.71	52.99
5	0.00	31.54	50.67	23.49	51.68	32.21

Table 4.2: Calculated Dose to the Contralateral Breast for all Treatment Plans

Section 2: T-test for Location/Depth of MOSFET

This test was performed by comparing the compensator and MLC data for each individual MOSFET for all of the plans for the medial field and then the lateral field. The results of the T-test are given in Table 4.3.

Medial Field					Lateral Field			
MOSFET #	Mean Dose for MLC	Mean Dose for Compensator	p value		MOSFET #	Mean Dose for MLC	Mean Dose for Compensator	p value
1	91.39	93.34	0.513		1	41.5	41.83	0.911
2	97.94	99.56	0.692		2	37.17	39.94	0.1
3	86.66	88.81	0.616		3	27.49	30.95	0.136
4	171.58	173.37	0.756		4	45.09	47.94	0.302
5	77.57	82.49	0.196		5	31.82	31.6	0.914

Table 4.3: T-test Results for the Depth of the MOSFET.

Looking at the data in Table 4.3, there is no p value less than 0.10 so there are not any significant values as a result of this test. That means that there is no difference at any depth from the compensator to the MLC method.

Section 3: T-test for Treatment Plans

This analysis was performed similar to that of the previous test except that now the treatment plans are being paired together. Treatment plan 1 for the MLC is being compared with treatment plan 1 for the compensator for the medial field and then again for the lateral field. Table 4.4 contains the paired T-tests for the treatment plans.

Medial Field				Lateral Field			
Treatment Plan	Mean Dose for MLC	Mean Dose for Compensator	p value	Treatment Plan	Mean Dose for MLC	Mean Dose for Compensator	p value
1	2.61	5.48	0.0081	1	0.56	1.24	0.4709
2	135.62	128.24	0.0262	2	35.84	36.91	0.3209
3	221.86	241.02	0.0002	3	49.61	58.12	0.0017
4	134.39	131.43	0.1095	4	32.34	27.31	0.0267
5	3.05	8.19	0.0326	5	63.29	66.99	0.1285
6	132.63	130.73	0.165	6	38.02	40.14	0.4327

Table 4.4: T-test Results for Treatment Plan.

The medial field shows that four out of the six treatment plans (plans 1, 2, 3 & 5) show a significant change in the mean dose. Out of the four plans, treatment plans 1, 3, and 5 show that the MLC delivers least dose to the contralateral breast. Plan 2 is the only one with a significant value that shows a lower dose for the compensator.

The lateral field shows that plans 3 and 4 are significant values. Plan 3 shows that MLC delivers the lower dose for this field and plan 4 shows that the compensator delivers the lower dose.

Section 4: T-test for the Field – Medial and Lateral

This test paired together the entire data for the MLC medial field and the compensator medial field as well as their respective lateral fields. The test tries to show a general

influence on the dose to the contralateral breast from the field for all the plans for each method.

Medial Field			Lateral Field		
Mean Dose for MLC	Mean Dose for Compensator	p value	Mean Dose for MLC	Mean Dose for Compensator	p value
105.03	107.52	0.1468	36.61	38.45	0.0618

Table 4.5: T-test Results for Each Individual Field

The data in Table 4.5 shows that there is a significant value for the lateral field. The values show that the dose from the MLC is less than the dose from the compensator.

Section 5: Overall T-test for All data for MLC and Compensator

The final T-test pairs all of the data for the MLC with all of the data for the compensator. The final test sees if there is an overall generalization that can be made about the dose to the contralateral breast for the two methods.

MLC vs Compensator		
Mean Dose for MLC	Mean Dose for Compensator	p value
70.82	72.99	0.0267

Table 4.6: T-test for Overall Comparison of MLC vs Compensator.

Table 4.6 shows that the test produced a significant result. The final test shows that the MLC delivers less dose to the contralateral than the compensator when all of the factors are included.

5. Conclusion

In general, the compensator did not reduce the external scatter dose to the contralateral breast as expected. There were a couple of exceptions for a treatment plan and a lateral field arrangement. However, it can be deduced from the statistical analyses that without further studies as to the exact nature of the exceptions that compensator does not reduce the dose to the contralateral breast. These studies need to inspect the characteristics of the treatment plans, gantry angles, patient qualities, and other factors that may give rise to these exceptions. A larger study with more measurements under each condition would be useful to make the statistical tests more powerful, but these initial findings are not promising as to the benefit of compensators for minimizing CLB dose.

Upon further inspection as to why the initial hypothesis failed, one possibility is that when any modulating material (i.e. wedge, compensator, etc.) is placed in the beam path, there is an increase in the amount of external scatter (Kelley 1996). These materials are also closer to the patient than the MLC. This closer proximity might allow for higher probability in the scattered photons to interact with the contralateral breast.

It is the final conclusion that the compensator does not reduce the contralateral dose as effectively as the MLC for most of the situations tested. Further studies need to be made to deduce the actual advantage of the select situations when the compensator did

overcome the MLC to ensure the validity of the data as well as the exact conditions that favored the compensator method.

6. References

1. Arriagada, R.; Le, M. G.; Rochard, F.; *et al*. Conservative treatment versus mastectomy in early breast cancer: Patterns of failure with 15 years of follow-up data. *J. Clin. Oncol.* **14**:1558-64; 1996.
2. Attix, F. Introduction to Radiological Physics and Radiation Dosimetry. John Wiley & Sons Inc. 1986.
3. Bhatnagar, A. K.; Brandner, E.; Sonnik, D.; *et al*. Intensity-modulated radiation therapy (IMRT) reduces the dose to the contralateral breast when compared to conventional tangential fields for primary breast irradiation: Initial report. *Cancer J.* **10**:381-5; 2004.
4. Boice, J. D.; Harvey, E. B.; Blettner, M.; *et al*. Cancer in the contralateral breast after radiotherapy for breast cancer. *N. Engl. J. Med.* **326**:781-5; 1992.
5. Fisher, B.; Anderson, S.; Redmond, C. K.; *et al*. Reanalysis and results after 12 years of follow-up in a randomized clinical trial comparing total mastectomy with lumpectomy with or without irradiation in the treatment of breast cancer. *N. Engl. J. Med.* **333**:1456-61; 1995.
6. Gao, X.; Fisher, S. G.; Emami, B. Risk of second primary cancer in the contralateral breast in women treated for early-stage breast cancer: A population-based study. *Int. J. Radiat. Oncol. Biol. Phys.* **56**:1038-45; 2003.
7. Goffman, T. E.; Miller, M.; Laronga, C.; *et al*. Shielding of the contralateral breast during tangential irradiation. *Am. J. Clin. Oncol.* **27**:436-9; 2004.
8. Hall, E. Radiobiology for the Radiologist. Lippincott Williams & Wilkins. Philadelphia. 2006.

9. Jacobson, J. A.; Danforth, D. N.; Cowan, K. H.; *et al*. Ten-year results of a comparison of conservation with mastectomy in the treatment of stage I and II breast cancer. *N. Engl. J. Med.* **332**:907-11; 1995.
10. Kelly, C. A.; Wang, X. Y.; Chu, J. C. H.; *et al*. Dose to contralateral breast: A comparison of four primary breast irradiation techniques. *Int. J. Radiat. Oncol. Biol. Phys.* **34**:727-32; 1996.
11. Khan, F. The Physics of Radiation Therapy. Lippincott Williams & Wilkins. Philadelphia. 2003.
12. Kurtz, J. M.; Almaric, R.; Brandone, H.; *et al*. Contralateral breast cancer and other second malignancies in patients treated by breast-conserving therapy with radiation. *Int. J. Radiat. Oncol. Biol. Phys.* **15**:277-84; 1988.
13. Muller-Runkel, R.; Kalokhe, U. P. Scatter dose from tangential breast irradiation to the uninvolved breast. *Radiology.* **175**:873-6; 1990.
14. Murshed, H. Clinical Fundamentals for Radiation Oncology Residents. Medical Physics Publishing. Wisconsin. 2006.
15. Obedian, E.; Fischer, D. B.; Haffty, B. G.; Second malignancies after treatment of early-stage breast cancer: Lumpectomy and radiation therapy versus mastectomy. *J. Clin. Oncol.* **18**:2406-12; 2000.
16. Sarrabayrouse, G.; Siskos, S. Radiation dose measurement using MOSFETs. Retrieved on: 5 June 2008. http://ieeexplore.ieee.org/xpls/abs_all.jsp?arnumber=685494.

17. Sohn, J. W.; Macklis, R.; Suh, J. H.; *et al*. A mobile shield to reduce scatter radiation to the contralateral breast during radiotherapy for breast cancer: Preclinical results. *Int. J. Radiat. Oncol. Biol. Phys.* **43**:1037-41; 1999.
18. van Dongen, J. A.; Voogd, A. C.; Fentiman, I. S.; *et al*. Long-term results of a randomized trial comparing breast-conserving therapy with mastectomy: European Organization for Research and Treatment of Cancer 10801 trial. *J. Natl. Cancer Inst.* **92**:1143-50; 2000.
19. Veronesi, U.; Salvadori, B.; Luini, A.; *et al*. Breast conservation is a safe method in patients with small cancer of the breast. Long-term results of three randomized trials on 1973 patients. *Eur. J. Cancer* **31A**:1567-9; 1995.